Secondary Structure of the Particle Associating Domain of Apolipoprotein B-100 in Low-Density Lipoprotein by Attenuated Total Reflection Infrared Spectroscopy

Erik Goormaghtigh,*,‡ Véronique Cabiaux,‡ Joëlle De Meutter,‡ Maryvonne Rosseneu,§ and Jean-Marie Ruysschaert‡

Laboratoire de Chimie Physique des Macromolécules aux Interfaces, Université Libre de Bruxelles, CP 206/2, Boulevard du Triomphe, B-1050 Bruxelles, Belgium, and St Jan Hospital, Bruges, Belgium

Received December 31, 1992; Revised Manuscript Received March 31, 1993

ABSTRACT: The secondary structure of the human low-density lipoprotein (LDL) apo B-100 fragment embedded in the lipid domain of the particle has been investigated by Fourier transform attenuated total reflection infrared spectroscopy (FTIR-ATR). The solvent-exposed region of the protein was hydrolyzed by using different proteases (α-chymotrypsin, trypsin, proteinase K) for incubation times varying between 24 min and 48 h. Analysis of the FTIR-ATR spectra after repurification of the digested LDL particle indicates the same trend for all the hydrolysis conditions tested: the peptides remaining associated with the particle are rich in β-sheet structure. Dichroism spectra reveal that at least part of the β-sheets is associated with the phospholipid component of the particle.

Low-density lipoproteins (LDL)[1] represent a major lipoprotein fraction and play an important role in the development of atherosclerotic lesions (Rudel et al., 1986). LDL are indeed able to transport plasma cholesterol to various tissues in which it can be deposited after interaction of LDL with cellular receptors (Brown & Goldstein, 1986a). Apo B-100 is present at the surface of the LDL particle and stabilizes the structure of the apolipoprotein–lipid particular complex (Atkinson & Small, 1986). The core of the LDL particle consists mostly of cholesterol esters (48% of the total lipid fraction) and of triacylglycerols (6%). This core is surrounded by a layer of phospholipid (34%) and unesterified cholesterol (12%). Knowledge of the secondary structure of the apo B-100 protein can contribute significantly toward the understanding of the assembly of the LDL particle.

β-Sheet structure has been identified in apo B-100 (Gotto et al., 1968), but no evidence for the presence of lipid-associated β-sheet structure has been reported. In a recent paper, we reported the secondary structure of apo B-100 in LDL investigated both by transmission and attenuated total reflection infrared spectroscopy. The amount of α-helix was found to be 21%, β-sheet 41%, β-turns 19%, and random 19% (Goormaghtigh et al., 1989). The rather large fraction of the protein adopting a β-sheet structure is in contrast with the common belief that stretches of proteins embedded in a hydrophobic environment always adopt an α-helical structure in order to fulfill hydrogen-bonding requirements. In the particular case of membrane proteins, most transmembrane regions adopt an α-helical structure [e.g., the photosynthetic complex of *Rhodopseudomona viridis* (Michel, 1982) and bacteriorhodopsin (Henderson et al., 1990)] with the notable exception of bacterial porins whose β-sheets form the backbone of the pore (Walian & Jap, 1990). The mode of association of apo B-100 with the LDL particle therefore remains to be resolved. Its high β-sheet content and the well-defined orientation of β-sheet structure with respect to the phospholipids (Goormaghtigh et al., 1989) suggest a strong interaction between the particle and β-sheet structure. Since it is generally admitted that the usual algorithms (Chou–Fasman, Garnier, etc.) fail to predict the structure of membrane embedded proteins (Wallace et al., 1986), and because circular dichroism (CD) is subject to artifacts due to scattering by particles or aggregated proteins, infrared spectroscopy remains one of the best tools to obtain information about the structure of membrane-associated proteins. ATR-FTIR is especially recommended to study membrane proteins since additional information on the orientation of the secondary structures with respect to the membrane plane can be obtained (Goormaghtigh & Ruysschaert, 1990). It has been successfully used in our laboratory to deal with numerous structural problems including membrane proteins (Goormaghtigh et al., 1987, 1990, 1991; Cabiaux et al., 1989; Hefele-Wald et al., 1990). Physical separation between the lipid-associated fraction of apo B-100 and the part of the protein exposed to the aqueous environment has been achieved by Yang et al. (1989) after proteolytic digestion of LDL by trypsin. In the present paper we have combined the latter proteolytic approach and the advantages of the IR-ATR methodology to define the structure and orientation of the peptides remaining associated with the LDL particle after various stages of proteolysis by trypsin, chymotrypsin, and proteinase K.

MATERIALS AND METHODS

Purification of LDL. Low-density lipoproteins (LDL) were isolated from fresh human plasma by sequential ultracentrifugation in a Beckman L5-65 ultracentrifuge (Rosseneu et al., 1981). The isolated LDL were then dialyzed at 4 °C against 0.15 M NaCl. The purity of the fractions was checked by agarose gel electrophoresis for contamination with other lipoproteins and by SDS–polyacrylamide gel electrophoresis in a 3–18% gradient for degradation and aggregation of apolipoprotein (apo) B-100. A single band (M_r ~500 000) was always observed.

The apo B-100 content of LDL and peptides were quantified by the method of Lowry et al. (1951) using bovine serum albumin as a standard.

Digestion of the LDL. LDL (260 μL; 4 mg of apo B-100/mL of buffer) was incubated with 10 μL of trypsin or

* To whom correspondence should be addressed.
‡ Université Libre de Bruxelles.
§ St. Jan Hospital.

[1] Abbreviations: apo, apolipoprotein; ATR, attenuated total reflection; CD, circular dichroism; FTIR, Fourier transform infrared spectroscopy; LDL, low-density lipoprotein; lb, lower band; ub, upper band.

0006-2960/93/0432-6104$04.00/0 © 1993 American Chemical Society

chymotrypsin (0.5 mg of enzyme/mL of buffer) or 25 μL of proteinase K (1 mg of enzyme/mL of buffer) at 37 °C for 48 h if not specified. Protease solutions were prepared by dissolution of the lyophilized protein into a 50 mM Tris HCl buffer containing 150 mM NaCl just prior to use. Digestion by a cocktail of proteases was carried out as follows: the LDL were first incubated for 2 h with 25 μL of 1 mg/mL papain, then for 16 h with 25 μL of 0.5 mg/mL proteinase K, then for 4 h with 25 μL of 0.5 mg/mL chymotrypsin, and finally for 12 h in the presence of 25 μL of 0.5 mg/mL chymotrypsin. For some experiments, the LDL were treated with 20 μL of phospholipase C (from *Bacillus cereus*) containing 80 units. In kinetic experiments PMSF (3 mM final concentration) was added to inhibit the proteolytic activity of proteinase K. For the other enzymes, the reaction was not stopped before running the repurification gradient (see below) since preliminary experiments have shown that this step was not necessary when 48-h incubation times are considered. The peptide fragments of apo B-100 associated to the lipid fraction of the particle were separated from the soluble peptides by ultracentrifugation on a sucrose gradient (2–30%) at 35 000 rpm, for 12 h at 10 °C. The fractions of the gradient were collected from the bottom of the tubes by carefully introducing a capillary tube at the bottom followed by aspiration at a flow rate of 0.4 mL/min. Fractions were dialyzed against a 10 mM Tris-HCl buffer, pH 7.6. Phospholipid determinations were performed with the colorimetric enzymatic kit from Boehringer (Mannheim) and protein dosages with the test of Lowry et al. (1951). Proteases and phospholipase C were all obtained from Sigma.

Infrared Spectroscopy. Attenuated total reflection infrared (ATR-FTIR) spectra were obtained on a Perkin-Elmer 1720X FTIR spectrophotometer equipped with a liquid nitrogen cooled MCT detector at a resolution of 2 cm^{-1}. A total of 256 scans were averaged for each measurement. Every four scans, reference spectra of a clean germanium plate were automatically recorded by a sample shuttle accessory and and ratio was calculated against the recently run sample spectra. No baseline correction was introduced since a blank made out of a lipid extract of LDL does not absorb in the region of amide I between 1700 and 1600 cm^{-1} before or after deuteration as shown previously (Goormaghtigh et al., 1989). The spectrophotometer was continuously purged with dry air. For polarization experiments, a Perkin-Elmer silver bromide polarizer was placed before the sample and before the reference plate. The internal reflection element was a germanium ATR plate (50 × 20 × 2 mm, Harrick EJ2121) with an aperture angle of 45° yielding 25 internal reflections. Measurements were carried out at 20 °C.

Thin films were obtained as described by Fringeli and Günthard (1981) by slowly evaporating 75 μL of the sample on one side of the ATR plate in a stream of nitrogen. Phospholipid films are not completely dehydrated by this procedure and have been shown to retain their physicochemical characteristics such as phase transition, lateral diffusion rate of the lipids, and area occupied/molecule (Levine & Wilkins, 1971; Clark et al., 1980; Tiede, 1985).

The ATR plate was then sealed in a universal sample holder (Perkin-Elmer 186-0354) and hydrated by flushing ^2H_2O-saturated N_2 (room temperature) for 3 h. Upon H/^{2}H exchange, the absorption band associated with the random secondary structure shifts from about 1655 to about 1642 cm^{-1}. This permits one to differentiate α-helical secondary structure from random secondary structure (Susi et al., 1967). To avoid recording spectra of material not included in the cavity of the universal sample holder, which has a controlled atmosphere, a 10-mm window was left open on the middle of the aperture of the ATR plate; the two side regions were masked by a thick Teflon sheet.

Secondary Structure Estimation. The determination of the secondary structure of soluble and membrane proteins by analysis of the shape of the deuterated amide band has been described previously (Goormaghtigh et al., 1990; Cabiaux et al., 1989).

Briefly, Fourier self-deconvolution was applied to increase the resolution of the spectra in the amide I′ region, which is the most sensitive region to the secondary structure of proteins. The self-deconvolution was carried out using a Lorentzian line shape for the deconvolution and a Gaussian line shape for the apodization, as described by Kauppinen et al. (1981).

Quantitative evaluation of the different components of amide I′ revealed by the self-deconvolution was performed by using a least-squares iterative curve fitting to fit Lorentzian line shapes to the spectrum between 1700 and 1600 cm^{-1}. Prior to curve fitting, a straight baseline passing through the ordinates at 1700 and 1600 cm^{-1} was subtracted. The spectrum arising from the lipid part of the system was found to be completely flat between 1700 and 1600 cm^{-1} and was therefore not subtracted.

The initial input parameters of the curve fitting were set as previously described (Goormaghtigh et al., 1990). In order to avoid introducing artifacts due to the self-deconvolution procedure, results were obtained from a fitting performed on a spectrum deconvoluted with $K = 1$.

The proportion of a particular structure was computed to be the sum of the area of all the fitted Lorentzian bands, having their maximum in the frequency region where that structure occurs, divided by the area of all the Lorentzian bands having their maxima between 1689 and 1615 cm^{-1}. The frequency regions for the different structures of deuterated proteins appear in Figure 4.

Orientation of the Secondary Structures. The theory on the determination of molecular orientations by infrared ATR has been reviewed by Fringeli and Günthard (1981) and ourselves (Goormaghtigh & Ruysschaert, 1990) and will not be described in more detail here.

When orientation was to be evaluated, additional spectra were recorded with parallel (0°) and perpendicular (90°) polarized incident light. Dichroism spectra are computed by subtracting the 0° polarized spectra from the 90° polarized spectra.

A larger absorbance at 90° (upward deviation on the dichroism spectrum) indicates a dipole oriented preferentially near a normal to the ATR plate. Conversely, a larger absorbance at 0° (downward deviation on the dichroism spectrum) indicates a dipole closer to the ATR plate. In the β-sheet structure, the dipole associated with amide I lays in the plane of the sheet, essentially parallel to the amide C=O axis.

RESULTS

When LDL are submitted to proteolytic digestion in the conditions described under Materials and Methods and reisolated on a sucrose density gradient, they migrate to a density which depends on the extent of protein removed from the particle as illustrated in Figure 1. In the absence of protease or in the presence of proteinase K inhibited by PMSF, the particle migrates to a density of 1.065. Treatment with proteinase K for 48 h results in a density of 1.025 and treatment with the protease cocktail for 48 h in a density of 1.015.

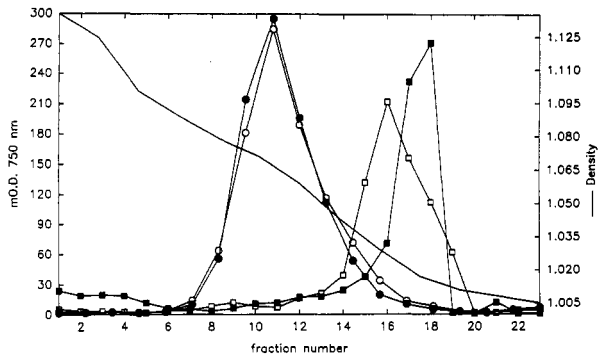

FIGURE 1: Phospholipid profiles for gradients used to repurify LDL after digestion by proteases under different conditions. The same amount of LDL (estimated from phospholipid dosage) was placed at the bottom of each gradient (fraction 1) and run at 35 000 rpm for 12 h at 10 °C. (○) Intact LDL; (●) incubation carried out after addition of PMSF prior to proteinase K addition. The symbols (□) and (■) refer, respectively, to LDL incubated in the presence of proteinase K and a cocktail of proteases (see Materials and Methods) for 48 h. The density was measured in each fraction by weighing of calibrated capillary tubing filled with an aliquot of each fraction. It is reported here as the continuous line.

Intermediate digestions yield intermediate densities. Protein profiles (data not shown) follow the lipid profiles except that after protease treatment an important peak remains at the bottom of the gradient (densities higher than 1.120) corresponding to the cleaved part of the protein. The peak fractions were pooled, dialyzed against 10 mM Tris-HCl buffer, and concentrated for infrared spectroscopy.

SDS–PAGE analysis of the peptides associated with the lipid particle after digestion by proteinase K for 48 h (not shown) indicates that no peptide of molecular mass higher than 41 500 Da is present. Other bands are visible at 36 700, 32 400, 28 700, 27 500, and 24 500 Da on a 7.5% gel. When an equal amount (according to phospholipid dosage) of intact LDL is incubated under the same conditions but in the absence of protease, no components of similar molecular mass are present but the main $M_r \simeq 500\,000$ band is very intense.

The spectrum of LDL particles is reported in Figure 2, panel A, curve a between 1800 and 1400 cm^{-1} after H/D exchange. The amide I′ (mainly C=O stretching of the amide groups of apo B-100) is located between 1690 and 1600 cm^{-1} with a maximum at 1622 cm^{-1} characteristic of a β-sheet structure. Unexchanged amide II is located between 1535 and 1550 cm^{-1}, and exchanged amide II (called amide II′) is found in the 1455-cm^{-1} region superimposed with the lipidic $\delta(CH_2)$ and H–O–D bending. The lipidic ester ν(C=O) band is present at 1733 cm^{-1}. After digestion by trypsin as described under Materials and Methods, the spectrum of the repurified particles is presented in Figure 2, panel A, curve c. At this stage of the digestion (33% of the protein removed), the shape of amide I′ resembles the shape of amide I′ of native LDL.

The IR spectrum of the part of the protein which has been removed from the LDL particle after proteolytic digestion can be computed (Figure 2, panel A, curve b) by subtracting the spectrum of the digested particles (Figure 2, panel A, curve c) from the spectrum of the native LDL (Figure 2, panel A, curve a), provided that the adequate subtraction coefficient can be estimated. Cardin and Jackson (1986) reported that some of the peptides released are able to interact with dimyristoylphosphatidylcholine vesicles to form high-density discoidal complexes. Since the lipid profiles reported in Figure 1 indicate that the lipid particles migrate as a single peak, we have chosen to use the lipid carbonyl band to evaluate the amount of LDL particle and to compute the subtraction coefficient. The area of the lipid ν(C=O) band located at 1733 cm^{-1} (hatched area) was used to calculate this coefficient. The resulting curve b presents no band near 1733 cm^{-1} as

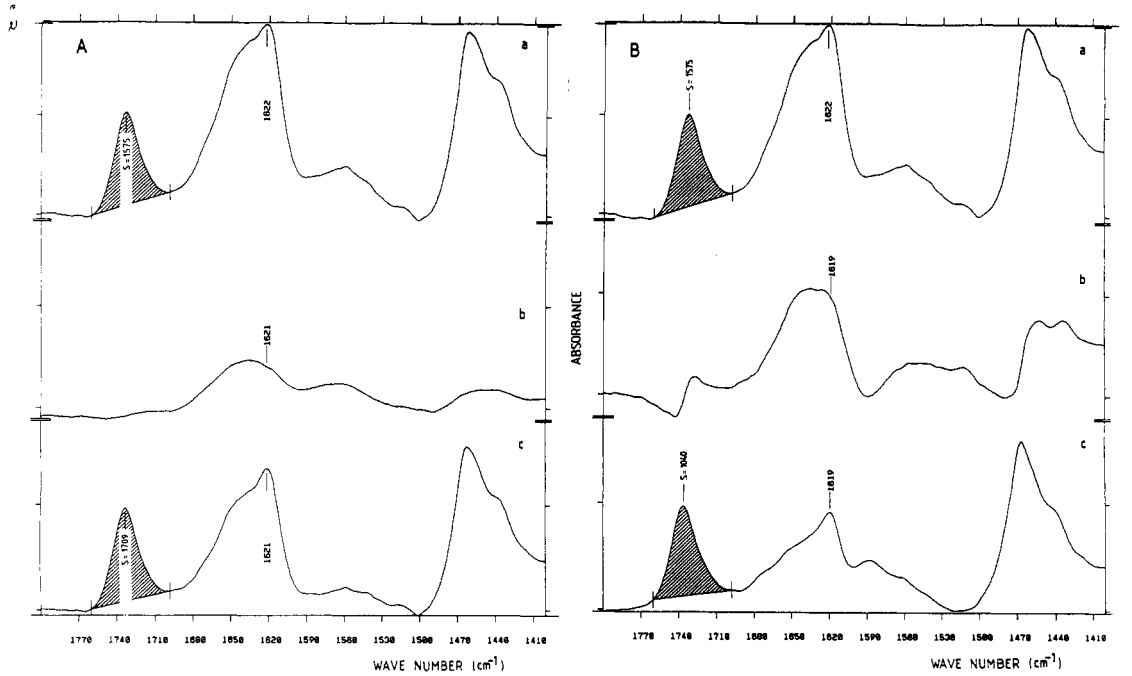

FIGURE 2: Infrared spectra of intact and digested LDL. (Panel A) deuterated (a) LDL and (c) LDL treated with trypsin for 48 h and repurified to remove the protease and released peptides as described under Materials and Methods; (b) released peptides after trypsinization for 48 h. This curve is obtained by difference between the native LDL (curve a) and the LDL-bound peptides (curve c) generated by the trypsin treatment. The scaling factor used for the difference is computed from the area of the lipid associated ν(C=O) (hatched on curve a and c) in order to zero the absorbance of the lipid ν(C=O) band in the 1720–1740-cm^{-1} frequency range. Spectra a and c have been rescaled so that on the figure the hatched areas are equal, i.e., represent the same amount of lipid. Curve b is on the same scale as curve c so that addition of curves b and c yields curve a. (Panel B) This part of the figure has been constructed exactly as described for panel A except that the sample (curve c) has been hydrolyzed for 5 h with proteinase K. The lower band obtained on the repurification gradient has been used.

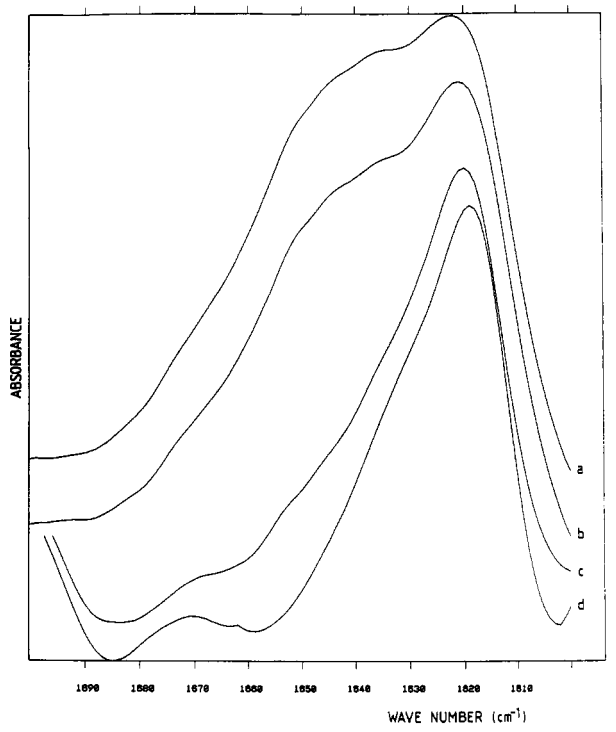

FIGURE 3: Infrared spectra in the region of amide I′ (between 1700 and 1600 cm^{-1}) of deuterated (a) native LDL, (b) LDL digested by trypsin (48 h), (c) LDL digested by proteinase K (48 h), and (d) LDL digested by a cocktail of proteases (48 h). The particles have been repurified as described under Materials and Methods. All the spectra have been rescaled to the sample amplitude. The OD range encompassing each curve are (a) 0.140, (b) 0.124, (c) 0.034, and (d) 0.017.

expected and is the spectrum of the part of the protein which has been removed from the particle. The shape of the amide I′ band is broad with a maximum in the 1640–1650-cm^{-1} range, i.e., in the α-helix and disordered frequency range of amide I′ but without the sharp maximum near 1622 cm^{-1} characteristic of high proportions of β-sheet structure. This suggests that more β-sheet remains associated with the lipid structure and more α-helix has been removed.

Different stages of the digestion were obtained by using either different proteases (α-chymotrypsin, trypsin, proteinase K, and a cocktail of them) or proteinase K with different incubation times. For several of the situations tested, hydrolysis of apo B-100 yields two bands in the density gradient used to repurify the digested LDL. Both bands were collected separately and are designated here as lower band (lb) and upper band (ub). The shape of amide I, normalized to an identical intensity, is compared for several of the conditions tested in Figure 3. It appears clearly from Figure 3 that digestion of the particles increases the relative amount of β-sheet component of amide I′ located around 1620 cm^{-1}. After the most extensive proteolytic digestions, only this component remains.

An analysis of the shape of amide I similar to that reported in Figure 2, panel A, is displayed in Figure 2, panel B, for digestion conditions in which about 50% of the protein has been removed (proteinase K, 5 h, lower band). The membrane-associated peptides now yield an amide I′ band with a greater β-sheet component, while the removed part of the protein yields a broad amide I′ band similar in shape but of course more intense than in the case of panel A.

In order to quantify the secondary structures, the amide I′ bands were analyzed as described under Materials and Method. An example of Fourier self-deconvolution and of the resulting

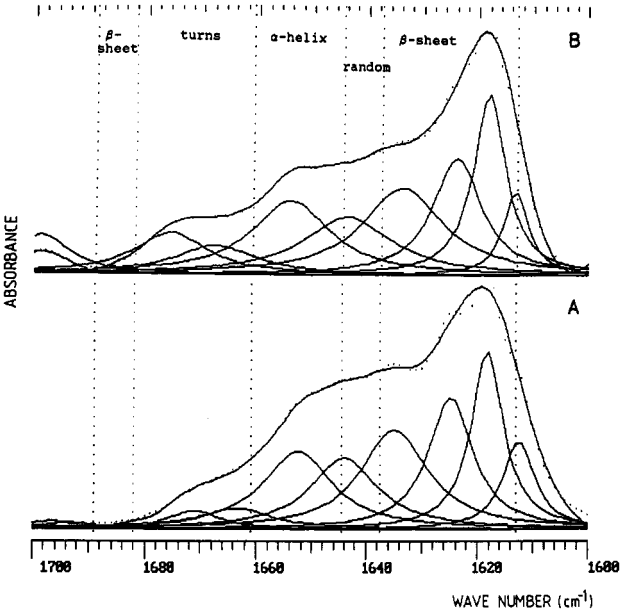

FIGURE 4: Final step of the secondary structure analysis [see Goormaghtigh et al. (1990) and Materials and Methods] of the samples described in the legend to Figure 2. (A) LDL digested by trypsin (48 h) and repurified; (B) LDL digested by proteinase K for 5 h and repurified. The assignment of the Lorentzian components to the different secondary structures is determined according to the frequency of their maximum. Each frequency domain is delimited by the vertical dotted lines and assigned to a secondary structure as labeled on the figure.

Table I: Secondary Structure of the apo B-100 Fraction Associated with the LDL Particle after Proteolytic Cleavage under Different Conditions[a]

protease	time		α-helix (%)	β-sheet (%)	disordered (%)	turns (%)	protein/lipid (%)
native	48 h		25	38	16	20	100
chymotrypsin	48 h		24	43	15	17	80
trypsin	48 h		20	55	17	7	67
proteinase K	48 h		6	72	0	12	11
cocktail	48 h		4	83	0	12	10
proteinase K	24 min	lb	16	54	20	10	74
		ub	10	55	18	17	65
	1 h	lb	16	55	18	10	64
	5 h	lb	16	56	14	14	47
		ub	17	52	18	12	56
	48 h		6	72	0	12	11

[a] When two bands, the lower band (lb) characterized by a higher density than the upper band (ub), appeared during the repurification of the digested LDL particle, both bands were collected and analyzed separately. The protein/lipid ratio was measured as described under Materials and Methods and normalized to 100% for the native LDL.

curve fitting appears in Figure 4 for the samples described in Figure 2. A similar analysis of the amide I′ obtained for the other proteolytic digestion conditions has been carried out, and the results are presented in Table I. Data reported in Table I confirm that the more the apo B-100 protein is hydrolyzed by proteases, the richer the particle becomes in β-sheet structure, indicating that the β-sheet structures are less accessible to the proteases.

A marked preferential orientation of the β-sheets in the films strongly suggests their association with the phospholipid component of the LDL (Goormaghtigh et al., 1989) since only the phospholipid may orient on the ATR plate because of their sheet-forming propensity. Figure 5 reports the dichroism spectra (see Materials and Methods) of native LDL and digested LDL. The dichroic spectra reported have been obtained by subtracting spectra recorded with a polarisation of 0° from spectra recorded with a polarization of 90° (not

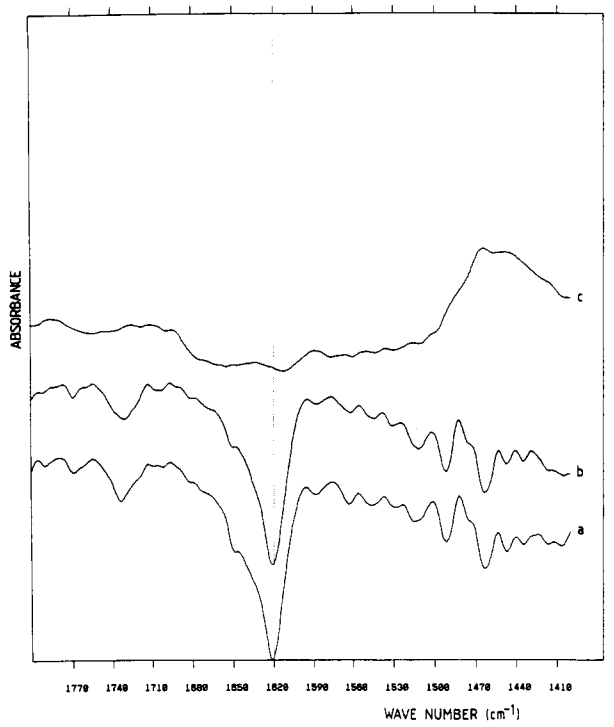

FIGURE 5: Dichroism spectra (90° polarization – 0° polarization) of deuterated sample of (a) native LDL, (b) LDL treated with trypsin (48 h) and then repurified as described under Materials and Methods, and (c) LDL treated for 5 h with proteinase K. The lower band of the repurification gradient has been used. The dichroism spectra have been rescaled as described under Results.

shown) with a coefficient chosen to zero the area of the lipid ν(C=O) at 1733 cm^{-1}. This coefficient was used because in the LDL particle the bulk of the lipid is not expected to be oriented and therefore should not display a different absorbance in the 90° and 0° polarized spectra. In order to provide comparable scales, the 90° polarized spectra were first rescaled to the same amplitude (not shown). For native LDL (Figure 5, curve a) a sharp maximum appears at 1620 cm^{-1} coinciding with the β-sheet component of amide I. This orientation is maintained when 33% of the protein is removed (Figure 5, curve b) but not after further digestion of the protein (Figure 5, curve c, and other data not shown).

DISCUSSION

The experiments described in this paper demonstrate that when proteases hydrolyze segments of apo B-100, presumably because they are not or less embedded in the lipid particle of the LDL, the β-sheet content of the LDL-associated protein increases while the content in α-helix, random, and turn structures decreases. The more advanced the hydrolysis, the richer the particle is in β-sheet structures. This is in agreement with the fact that peptides released after proteolytic cleavage have been shown previously to have a high content of α-helix and little β-sheet structure (Cardin & Jackson, 1986). The fraction of apo B-100 associated with the particle after extensive proteolytic treatment contains almost exclusively β-sheet structure according to the present data. It must, however, be stressed that our data do not preclude the presence of α-helices in the lipid region of the LDL. Indeed the helical component disappears only after long incubation times (48 h) and with high concentrations of proteases, possibly by a mechanism such as that described by Dumont et al. (1985).

The present work is based on three assumptions: (1) the proteolytic activity is supposed to be limited to the part of the protein protruding from the lipid layer surrounding the LDL particle; (2) the proteases used are rather nonspecific; and (3), the structure of the protein remaining associated to the particle is not modified by the protease treatment and the purification step.

The first assumption seems reasonable in view of the results of previous studies: a proteolytic approach to isolate the membrane-embedded fragments of membrane proteins has been used for bacteriorhodopsin (Gerber et al., 1977; Dumont et al., 1985), Na^+K^+-ATPase (Ovchinnikov et al., 1986), *Neurospora crassa* plasma membrane H^+-ATPase (Rao et al., 1991), and apo B-100 in LDL (Yang et al., 1989), to quote only a few, and has demonstrated that proteases such as trypsin or proteinase K limit their action to the part of the protein protruding from the membrane. The similar approach described in this paper for LDL requires that the proteases used are restricted to the outside of a particle which is limited by a phospholipid monolayer, a structure somewhat different from the usual phospholipid structure found in vesicles. In view of the similarities of phospholipid structure and packing in different model membranes [monolayers at the air–water interface (Jones, 1975; Tiede, 1985; Chapman, 1975), hydrated multibilayers (Tiede, 1985), bilayers in vesicles and LDL (Vauhkonen et al., 1989)] as indicated by identical phase transition temperature and lateral diffusion coefficients, it can be expected that the phospholipid monolayer surrounding the LDL particles presents a barrier for these proteases as efficient as the bilayer of the phospholipid membranes. The problem of whether or not the proteases used present some specificities for a given secondary structure can be partially answered by noting that when other membrane proteins are treated by the same proteases under the same experimental conditions, α-helices predominate in the membrane after elimination of released peptides [e.g., bacteriorhodopsin (Dumont et al., 1985) and Na^+K^+-ATPase (Ovchinnikov et al., 1988)]. Moreover, the same trend is observed here (Table I) for the different proteases, leaving little doubt that rather nonspecific cleavages occur.

The absence of marked conformational change in the membrane-associated peptides after protease treatment and purification is a fundamental assumption in this paper. Protein denaturation and/or aggregation (upon heating for instance) favors the formation of β-sheet structures characterized in infrared spectroscopy by low-frequency components in amide I. Whether or not protein denaturation and/or aggregation could contribute to the low-frequency β-sheet structure observed is therefore a matter of concern. Yet, the following arguments indicate that the low-frequency β-sheet component is not due to denaturation/aggregation: (1) the low-frequency β-sheet component is already present in the intact protein. It does not appear during the manipulations of the LDL. (2) The mere incubation of LDL under conditions similar to the digestion conditions but in the absence of protease does not modify the secondary structure of the protein as assessed by IR. Denaturation/aggregation should therefore be specifically induced by the protease. (3) The embedding of the protein studied in a hydrophobic environment should protect it against the effects of proteolytic degradation restricted to the aqueous phase. In fact because hydrophobic forces govern the folding of proteins, it is expected that the structure of lipid-embedded protein segments is not affected by the part of the protein protruding from the particle into the aqueous phase.

The low frequency of the β-sheet component near 1622 cm^{-1} is unusual for soluble and membrane proteins studied so far, as discussed previously (Cabiaux et al., 1989). Yet it is

found for diphtheria toxin at low pH where a low-frequency β-sheet component represents about 24% of the amide I absorbance (Cabiaux et al., 1989) and in lipophilin, which displays a prominent peak at 1621 cm^{-1} which accounts for approximately 30% of amide I absorbance (Surewicz et al., 1987). Several well-characterized β-sheet peptides also display low-frequency β-sheet bands (Chirgadze & Neveskaya, 1976). It is therefore likely that the low-frequency β-sheet components have to be assigned to a β-sheet structure with strong hydrogen bonds. In the case of apo B-100, strengthening of the hydrogen bonds could be favored by the hydrophobic environment within the particles. Recent investigation indicates that even severe oxidation of apo B-100 does not modify its secondary structures as seen by ATR-FTIR spectroscopy (Vanderyse et al., 1992). It can therefore be ruled out that oxidation plays a role in the nature of the 1622-cm^{-1} band.

It must be kept in mind when reading Table I that quantitative determination of secondary structures by infrared spectroscopy is limited by a number of valid reasons (Goormaghtigh et al., 1993; Torii & Tasumi, 1993; Wilder et al., 1992; Surewicz et al., 1993). However, in the present case the large frequency separation between the α-helix component and the β-sheet component allows a clear assignment. Considering an accuracy of 8% on these structures (Goormaghtigh et al., 1990) seems therefore a conservative option. The secondary structure evaluation supposes the random structure to have completed the H/D exchange. In such conditions its contribution to amide I shifts from ~1655 cm^{-1} where it is superimposed to the α-helix component to ~1642 cm^{-1}. Since only the random structure must be completely exchanged prior to secondary structure evaluation, we expect the necessary deuteration time to be in the range of a few minutes. The method of secondary structure evaluation was successfully tested without taking into account the degree of deuteration reached (Goormaghtigh et al., 1990). However, we found it useful to establish that the secondary structure evaluation does not depend on the deuteration time (see Supplementary Material).

The presence of a polarization of the spectra yields information about the lipid–protein association. As it has been elaborated upon before (Goormaghtigh et al., 1989), the strong 0° polarization of the β-sheet component of amide I′ indicates an association with the phospholipids surrounding the LDL which are the only constituent of the particle able to orient on the ATR plate. Data reported here indicate that, beyond a certain extent of protein digestion (between 30% and 50%), the orientation is completely lost. After long incubation times in the presence of the protease, the part of apo B-100 associated with the outer phospholipid shell of the LDL may be completely digested, and only the domain of the protein more deeply embedded in the hydrophobic region of the particle is left. Since the latter molecules cannot form oriented layers on the ATR plate, the associated β-sheet cannot be oriented. A simple explanation for the loss of orientation, therefore, is that two classes of β-sheet exist, one associated with the outer phospholipid layer and another more deeply embedded within the core of the LDL. This is, however, no more than a hypothesis since other possible explanations can be put forward, for instance, a complete restructuring of the lipid–protein association.

The results presented here suggest that β-sheet forms the major structure of apo B-100 associated with the LDL lipids. The location of the β-sheet structure inside the LDL particles is confirmed by their rather slow H/D exchange rate reported by Herzyk et al. (1987). Yang et al. (1989) separated apo B-100 tryptic peptides on the basis of their affinity for sonicated dimyristoylphosphatidylcholine vesicles. CD analysis of these lipid–protein complexes revealed a high content of random structure. A possible explanation for the discrepancy with the present results is that the peptides which were able to reassociate with the phospholipid bilayer in the work of Yang et al. are different from the peptides remaining associated with the LDL particle isolated in our study. Alternatively, the peptides recovered by Yang et al. were not able to recover their original structure after transfer into a phospholipid bilayer.

In contrast to the other apolipoproteins (apo A-1, A-2, A-4, E, etc.) apo B-100 is strongly associated to the lipid part of the particle, and no exchange of the protein between particles can occur. The present paper establishes that β-sheet structures are deeply associated within the lipid region of the LDL. The way β-sheets accommodate this environment is certainly different from the way β-sheets cross a lipid bilayer to form a pore in bacterial porins (Walian & Jap, 1990; Weiss et al., 1991) and remains to be elucidated.

ACKNOWLEDGMENT

J. De Meutter was an IRSIA fellow (Belgium), and E. Goormaghtigh is Research Associate of the National Fund for Scientific Research (Belgium).

SUPPLEMENTARY MATERIAL AVAILABLE

Two figures showing the kinetics of hydrogen/deuterium exchange and the effect of the deuteration extent on the secondary structure evaluation (4 pages). Ordering information is given on any current masthead page.

REFERENCES

Atkinson, D., & Small, S. M. (1986) *Annu. Rev. Biophys. Chem. 15*, 403–456.

Brown, M. S., & Goldstein, J. L. (1986a) *Ann. N.Y. Acad. Sci. 454*, 178–182.

Cabiaux, V., Brasseur, R., Wattiez, R., Falmagne, P., Ruysschaert, J. M., & Goormaghtigh, E. (1989) *J. Biol. Chem. 264*, 4928–4939.

Cardin, A. D., & Jackson, R. L. (1986) *Biochim. Biophys. Acta 877*, 366–371.

Chapman, D. (1975) *Q Rev. Biophys. 8*, 185–235.

Chirgadze, Y. N., & Neveskaya, N. A. (1976) *Biopolymers 15*, 607–625.

Clark, N. A., Rothschild, K. J., Luippold, D. A., & Simon, B. A. (1980) *Biophys. J. 31*, 65–96.

Dumont, M. E., Trewhella, J., Engelman, D. M., & Richards, F. M. (1985) *J. Membr. Biol. 88*, 233–247.

Fringeli, U. P., & Günthard, H. H. (1981) in *Membrane Spectroscopy* (Grell, E., Ed.) pp 270–332, Springer Verlag, New York.

Gerber, G. E., Gray, C. P., Wildenauer, D., & Korana, H. G. (1977) *Proc. Natl. Acad. Sci. U.S.A. 74*, 5426–5430.

Goormaghtigh, E., & Ruysschaert, J. M. (1990) in *Molecular Description of Biological Components by Computer Aided Conformational Analysis* (Brasseur, R., Ed.) pp 285–329, CRC Press, Boca Raton, FL.

Goormaghtigh, E., Brasseur, R., Huart, P., & Ruysschaert, J.-M. (1987) *Biochemistry 26*, 1789–1794.

Goormaghtigh, E., De Meutter, J., Vanloo, B., Brasseur, R., Rosseneu, M., & Ruysschaert, J. M. (1989) *Biochim. Biophys. Acta 1006*, 147–150.

Goormaghtigh, E., Cabiaux, V., & Ruysschaert, J. M. (1990) *Eur. J. Biochem. 193*, 409–420.

Goormaghtigh, E., De Meutter, J., Cabiaux, V., Szoka, F., & Ruysschaert, J. M. (1991a) *Eur. J. Biochem. 195*, 421–429.

Goormaghtigh, E., Vigneron, L., Knibiehler, M., Lazdunski, C., & Ruysschaert, J. M. (1991b) *Eur. J. Biochem. 202*, 1299–1305.
Goormaghtigh E., Cabiaux V., & Ruysschaert J. M. (1993) *Subcell. Biochem.* (in press).
Gotto, A. M., Levy, R. I., Jr., & Frederickson, D. S. (1968) *Proc. Natl. Acad. Sci. U.S.A. 60*, 1436–1439.
Hefele-Wald, J., Goormaghtigh, E., De Meutter, J., Ruysschaert, J. M., & Jonas, A. (1990) *J. Biol. Chem. 275*, 20044–20050.
Henderson, R., Baldwin, J. M., Ceska, T. A., Zemlin, F., Beckmann, E., & Downing, K. H. (1990) *J. Mol. Biol. 213*, 899–906.
Herzyk, E., Lee, D. C., Dunn, R. C., Bruckdorfer, K. R., & Chapman, D. (1987) *Biochim. Biophys. Acta 992*, 145–154.
Jones, M. N. (1975) *Biological Interfaces*, pp 35–65, Elsevier, Amsterdam.
Kalnin, N. N., Baikalov, I. A., & Venyaminov, S. Y. (1990) *Biopolymers 30*, 1273–1280.
Kauppinen, J. K., Moffat, D. J. Cameron, D. G., & Mantsch, H. H. (1981) *Appl. Opt. 20*, 1866–1879.
Levine, Y. K., & Wilkins, M. H. F. (1971) *Nature 230*, 69–73.
Lowry, O. H., Rosenbrough, N. J., Levin, A. L., & Randall, R. J. (1951) *J. Biol. Chem. 193*, 265–275.
Michel, H. (1982) *J. Mol. Biol. 158*, 567–572.
Ovchinnikov, Y. A., Modyanov, N. N., Broude, N. E., Petrukhin, K. E., Grishin, A. V., Arzamazova, N. M., Aldanova, N. A., Monastyrskaya, G. S., & Sverdlov, E. D. (1986) *FEBS Lett. 201*, 237–245.
Ovchinnikov, Y. A., Arystarkhova, E. A., Arzamazova, N. M., Dzhandzhugazyan, K. N., Efremov, R. G., Nabiev, I. R., & Modyanov, N. N. (1988) *FEBS Lett. 227*, 235–239.
Rao, S., Hennessey, J., & Scarborough, G. A. (1991) *J. Biol. Chem. 266*, 14740–14746.
Rosseneu, M., Vinaison, N., Vercaemst, R., De Keergieter, W., & Belpaire, F. (1981) *Anal. Biochem. 116*, 204–210.
Rudel, L. L., Parks, J. S., Johnson, F. L., & Babiak, J. (1986) *J. Lipid Res. 27*, 465–474.
Surewicz, W. K., & Mantsch, H. H. (1988) *Biochim. Biophys. Acta 952*, 115–1130.
Surewicz, W. K., Moscarello, M. A., & Mantsch, H. H. (1987) *J. Biol. Chem. 262*, 8598–8602.
Surewicz W. K., Mantsch H. H., & Chapman D. (1993) *Biochemistry 32*, 389–394.
Susi, H., Timasheff S. N., & Stevens, L. (1967) *J. Biol. Chem. 242*, 5460–5466.
Tiede, D. M. (1985) *Biochim. Biophys. Acta 811*, 357–379.
Torii H., & Tasumi M. (1992) *J. Chem. Phys. 96*, 3379–3387.
Vanderyse, L., Devreese, A. M., Baert, J., Vanloo, B., Lins, L., Ruysschaert, J. M., & Rosseneu, M. (1992) *Atherosclerosis 97*, 187–199.
Vauhkonen, M., Sassaroli, M., Somerharju, P., & Eisinger, J. (1989) *Eur. J. Biochem. 186*, 465–471.
Walian, P. J., & Jap, B. K. (1990) *J. Mol. Biol. 215*, 429–438.
Wallace, B. A., Cascio, M., & Hielke, D. L. (1986) *Proc. Natl. Acad. Sci. U.S.A. 83*, 9423–9427.
Weiss, M. S., Kreusch, A., Schiltz, E., Nestel, U., Welte, W., Weckesser, J., & Schulz, G. E. (1991) *FEBS Lett. 280*, 379–382.
Wilder C. L., Friedrich A. D., Potts R. O., Daumy G. O., & Francoeur M. L. (1992) *Biochemistry 31*, 27–31.
Yang, C. Y., Kim, T. W., Pao, Q., Chan, L., Knapp, R. D., Gotto, A. M., & Pownall, H. J. (1989) *J. Protein Chem. 8*, 689–699.